MDPI

Article

Proposed Approach for Modelling the Thermodynamic Behaviour of Entrapped Air Pockets in Water Pipeline Start-Up

Dalia M. Bonilla-Correa [1], Oscar E. Coronado-Hernández [2], Alfonso Arrieta-Pastrana [2], Modesto Pérez-Sánchez [3,*] and Helena M. Ramos [4]

1   Facultad de Ciencias Exactas y Naturales, Universidad de Cartagena, Cartagena 131001, Colombia
2   Instituto de Hidráulica y Saneamiento Ambiental, Universidad de Cartagena, Cartagena 131001, Colombia
3   Departamento de Ingeniería Hidráulica y Medio Ambiente, Universitat Politècnica de València, 46022 Valencia, Spain
4   Civil Engineering, Architecture and Environment Department, CERIS, Instituto Superior Técnico, University of Lisbon, 1049-001 Lisbon, Portugal; helena.ramos@tecnico.ulisboa.pt
*   Correspondence: mopesan1@upv.es

Abstract: Water utilities are concerned about the issue of pipeline collapses, as service interruptions lead to water shortages. Pipeline collapses can occur during the maintenance phase when water columns compress entrapped air pockets, consequently increasing the pressure head. Analysing entrapped air pockets is complex due to the necessity of numerically solving a system of differential equations. Currently, water utilities need more tools to perform this analysis effectively. This research provides a numerical solution to the problem of entrapped air pockets in pipelines which can be utilised to predict filling operations. The study develops an analytical solution to examine the filling process. A practical application is shown, considering a 600 m long pipeline with an internal diameter of 400 mm. Compared with existing mathematical models, the results of the new analytical equations demonstrate their effectiveness as a new tool for computing the main hydraulic and thermodynamic variables involved in this issue.

1. Introduction

A pipeline start-up is an ordinary operation in water distribution systems that water utilities must conduct [1,2]. This operation represents a complex modelling problem, requiring an appropriate combination of thermodynamic and hydraulic formulations to describe the air and water phases [3,4]. Additionally, several pipeline ruptures have occurred due to the unsuitable performance of this operation. Ruptures can be provoked during this process's initial stages, since air pockets are rapidly compressed, increasing the air pocket pressure inside hydraulic installations [3,5].

The modelling of this problem has been approached using one-dimensional (1D), two-dimensional (2D), and three-dimensional (3D) numerical resolution schemes [6–9]. The elastic-column (ECM) and rigid-column (RCM) models have been extensively used to study the behaviour of water movement, employing a system composed of differential equations [10–12]. Both models provide similar results, since the elasticity of the air phase is much greater than the pipe wall's elasticity and the water phase's volumetric changes [3]. Several researchers have recently undertaken the formulation using these models.

Two-dimensional and three-dimensional models have been addressed using computational fluid dynamics (CFD), employing the commercial packages ANSYS and Open-FOAM [8,13]. These models have been primarily used to explore complex scenarios where 1D models have limitations related to the shapes of air-water interfaces [14]. One-dimensional, two-dimensional, and three-dimensional models provide similar water velocity, air pocket pressure, and the length of water column pulses when air–water interfaces

coincide perpendicularly with the main direction of pipelines. However, when air–water interfaces tend towards the shape of bubble flow, plug, stratified wave, or stratified smooth flow, only 2D and 3D CFD models can adequately simulate the behaviour of the leading hydraulic and thermodynamic variables in water installations during this process.

During the occurrence of start-up processes, two instances are particularly relevant. The first corresponds to the process's end, as water utilities can compute the total duration for cleaning or maintenance manoeuvres on water installations. The investigation conducted by Bonilla-Correa et al. (2023) [15] provided an explicit formulation to compute the final time of this process. The second instance is marked by the peak value of an air pocket pressure pulse, which must be considered to determine if the pipe's resistance class is sufficient to prevent a rupture.

According to various investigations, this peak value usually occurs during the initial stages, as rapid compression of air pockets occurs at this time [3,5]. To compute this maximum value, a complex system of differential-algebraic equations needs to be solved, taking into account the momentum equation for modelling the water phase, the air–water interface formulation, and the air phase's polytropic formulation [12]. Water utilities require practical tools for rapidly computing these values, as they must analyse many water installations [16]. A semi-empirical equation has been previously proposed by Tijsseling et al. (2015) [17].

Although 1D models require less computational time than 2D and 3D CFD, they necessitate implementing a complex system of differential equations that must be formulated based on the specific water pipeline configurations. No commercial software is available to predict filling operations in water distribution systems.

This research demonstrates an analytical equation [18,19] for modelling the thermodynamic behaviour of air pockets in a single water pipeline start-up. The equation considers the physical equations governing the behaviour of this process. Engineers can use this equation to compute the maximum value in air pocket pressure in water pipelines during this hydraulic event. The demonstrated equation is valid until the instance of backflow occurrence. A practical application is conducted considering a pipe length of 600 m and an internal diameter of 400 mm.

The results show that the analytical equation provides a similar maximum value in air pocket pressure compared to the numerical resolution of the differential-algebraic equations system, confirming its adequacy for computing this maximum value. A sensitivity analysis using different mathematical approximations was conducted to demonstrate the robustness of the analytical approach.

2. Materials and Methods

Starting-up a water pipeline is a standard procedure for cleaning and maintenance by water utilities. This process begins with the pipeline at rest ($v = 0$) because the regulating valves are closed. When a valve operation begins, air pockets are compressed, increasing air pocket pressure. Ensuring that an air pocket pressure does not exceed a pipe's resistance class value is crucial if no air valves exist. Figure 1 shows the main hydraulic and thermodynamic variables involved when a system is at rest. L_0 corresponds to the initial length of a water column, x_0 is the initial air pocket size, p_0^* is the pressure supplied by a tank or a pumping station, and L_T is the total pipe length.

When a regulating valve is opened, a water column fills a hydraulic installation, causing the air–water interface to change over time. Since no air valve is located at the highest point of the water installation, the air pocket is rapidly compressed. At the end of the transient event, the air pocket remained inside the system.
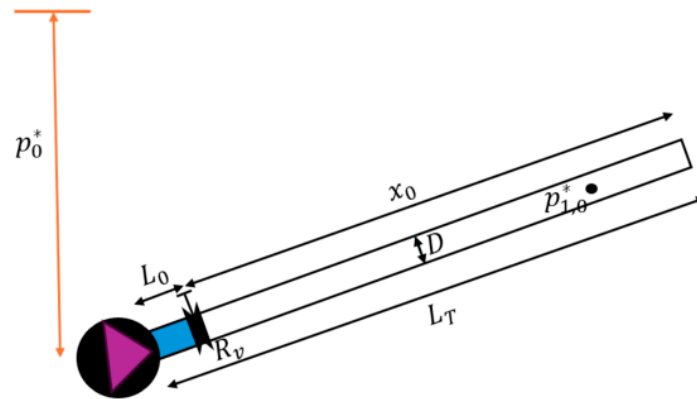
Figure 1. Water pipeline start-up scheme.

2.1. Current Mathematical Model

A system of differential equations has been defined to analyse the problem of filling processes in single pipelines. The ECM and RCM yield similar results because the pipe thickness and the volumetric changes of the water are not significant; the elasticity of the air phase is much higher in comparison. These models have been previously developed by Zhou et al. (2013) [20] and Coronado-Hernández at al. (2019) [21]. Both models assume that an air–water interface is perpendicular to the main direction of a pipe. The RCM is used for describing the movement of a water column in a filling pipe process, as follows:

- The air–water interface formulation assumes that this front is perpendicular to the main direction of a pipe system [1,16]:

$$\frac{dL}{dt} = v,$$

(1)

where v = water velocity, and L = length of a water column at time t.

- The polytropic law describes the air behaviour:

$$p_1^* x^k = p_{1,0}^* x_0^k,$$

(2)

where p_1^* = air pocket pressure, $p_{1,0}^*$ = initial air pocket pressure, x = air pocket size at time t, and k = polytropic coefficient. Considering that the air pocket size can be calculated as $x = L_T - L$, then the air pocket pressure at time t is providing by:

$$p_1^* = \frac{p_{1,0}^* x_0^k}{(L_T - L)^k},$$

(3)

Usually, an air pocket pressure begins at atmospheric conditions ($p_{1,0}^* = p_{atm}^* = 101{,}325$ Pa). The RCM can be used to describe the water phase movement [15,22].

$$\frac{dv}{dt} = \frac{p_0^* - p_1^*}{\rho L} + g\sin\theta - \frac{f}{2D}v|v| - \frac{R_v g A^2}{L}v|v|,$$

(4)

where f = friction factor, D = internal pipe diameter, θ = longitudinal slope, R_v = resistance coefficient of a regulating valve, g = gravitational acceleration, ρ = water density, and A = cross-sectional area of a pipe.

By plugging Equation (3) into Equation (4):

$$\frac{dv}{dt} = \frac{p_0^*}{\rho L} - \frac{p_{1,0}^* x_0^k}{\rho L (L_T - L)^k} + g\sin\theta - \frac{f}{2D}v|v| - \frac{R_v g A^2}{L}v|v|,$$

(5)

The initial conditions of a filling water process begin at rest which implies that $v(0) = 0$; $L(0) = L_0$; $p_1^*(0) = p_{atm}^*$; $x(0) = L_T - L(0) = x_0$.

2.2. Proposed Approach

This section presents the proposed approach developed in this research. The objective is to create a numerical-analytical solution that can be used for computing the maximum value of the air pocket pressure head without solving the complex system composed by Equations (1) and (5).

The assumptions underlying the proposed approach are outlined as follows:

- The pressure at the pipeline inlet is assumed to remain constant throughout filling operations.
- The air–water interface is analysed under the assumption of piston flow.

  The air phase's behaviour is modelled using the polytropic law.

- The RCM is utilised to describe the behaviour of the water phase.
- The operation of regulating valves is considered to be instantaneous.

2.2.1. Analytical Solution

Considering the chain rule for Equations (1) and (5), then $\frac{dv}{dL} = \frac{\frac{dv}{dt}}{\frac{dL}{dt}}$. Thus, it is possible to demonstrate that:

$$v\frac{dv}{dL} = \frac{p_0^*}{\rho L} - \frac{p_{atm}^* x_0^k}{\rho L (L_T - L)^k} + g\, sin\, \theta - \frac{f}{2D}v|v| - \frac{R_v g A^2}{L}v|v|, \tag{6}$$

In this case, $\frac{d(v^2)}{dL} = 2v\frac{dv}{dL}$. Thus:

$$\frac{d(v^2)}{dL} = \frac{2p_0^*}{\rho L} - \frac{2p_{atm}^* x_0^k}{\rho L (L_T - L)^k} + 2g\, sin\, \theta - \frac{f}{D}v|v| - \frac{2R_v g A^2}{L}v|v|, \tag{7}$$

The maximum value of the air pocket pressure in a rapid filling process without air valves occurs when the movement of the water column reaches zero velocity during the transient event. In this sense, considering that $v \geq 0$, then:

$$\frac{d(v^2)}{dL} = \frac{2p_0^*}{\rho L} - \frac{2p_{atm}^* x_0^k}{\rho L (L_T - L)^k} + 2g\, sin\, \theta - \frac{f}{D}v^2 - \frac{2R_v g A^2}{L}v^2, \tag{8}$$

Using $z = v^2$ and reorganizing terms in Equation (8):

$$\frac{d(z)}{dL} + \left(\frac{f}{D} + \frac{2R_v g A^2}{L}\right)z = 2\frac{p_0^*}{\rho L} - \frac{2p_{atm}^* x_0^k}{\rho L (L_T - L)^k} + 2g\, sin\, \theta, \tag{9}$$

where z = square of v.

Equation (9) is a first-order linear formula that can be solved using the integrating factor $e^{h(L)} = e^{\frac{f}{D} L + 2R_v g A^2 (lnL)}$. $h(L)$ is a function of friction factor, internal pipe diameter, resistance coefficient of a regulating valve, gravitational acceleration, cross-sectional area, and the variable of integration (s). The value of $h(L) = \int \frac{f}{D} + \frac{2R_v g A^2}{s} ds$.

Multiplying the left and right sides of Equation (9) by the integrating factor, then:

$$e^{h(L)}\left(\frac{d(z)}{dL} + \left(\frac{f}{D} + \frac{2R_v g A^2}{L}\right)z\right) = \left(e^{\frac{f}{D} (L)}(L)^{2R_v g A^2}\right)\left(2\frac{p_0^*}{\rho L} - \frac{2p_{atm}^* x_0^k}{\rho L (L_T - L)^k} + 2g\, sin\, \theta\right), \tag{10}$$

By organising terms and simplifying, it is possible to obtain:

$$\frac{d\left(ze^{h(L)}\right)}{dL} = \left(e^{\frac{f}{D}(L)}(L)^{2R_vgA^2}\right)\left(2\frac{p_0^*}{\rho L} - \frac{2p_{atm}^*x_0^k}{\rho L(L_T - L)^k} + 2g\,sin\,\theta\right),\tag{11}$$

By integrating Equation (11) with limits from L_0 and L, where $L \in (L_0, L_T)$, and $v(S) > 0$ for all $S \in (L_0, L]$, then:

$$ze^{h(L)} = \int_{L_0}^{L}\left(e^{\frac{f}{D}(S)}(S)^{2R_vgA^2}\right)\left(2\frac{p_0^*}{\rho S} - \frac{2p_{atm}^*x_0^k}{\rho S(L_T - S)^k} + 2g\,sin\,\theta\right)dS,\tag{12}$$

By solving for z, thus:

$$z = \left(\frac{1}{e^{\frac{f}{D}L}L^{2R_vgA^2}}\right)\int_{L_0}^{L}\left(e^{\frac{f}{D}(S)}(S)^{2R_vgA^2}\right)\left(2\frac{p_0^*}{\rho S} - \frac{2p_{atm}^*x_0^k}{\rho S(L_T - S)^k} + 2g\,sin\,\theta\right)dS,\tag{13}$$

The water velocity (v) is yielding by the expression, as follows:

$$v(L) = \sqrt{\left(e^{\frac{f}{D}L}L^{2R_vgA^2}\right)^{-1}\int_{L_0}^{L}\left(e^{\frac{f}{D}(S)}(S)^{2R_vgA^2}\right)\left(2\frac{p_0^*}{\rho S} - \frac{2p_{atm}^*x_0^k}{\rho S(L_T - S)^k} + 2g\,sin\,\theta\right)dS,}\tag{14}$$

which is valid from values of $v(L) > 0$.

Equation (14) corresponds to an analytical resolution that involves an integral that must be solved numerically, as presented below.

2.2.2. Numerical Resolution

The analytical solution presented in Section 2.2.1 contains a term that must be solved numerically using Simpson's 1/3 rule. This simple method approximates the integrand with a quadratic polynomial function [23], yielding a fifth-order error. Its approximation is employed because a water velocity (v) in the $L - v$ plane is a smooth concave function, making the method suitable for quadratic functions. Additionally, Simpson's 3/8 rule can be used, as it employs cubic polynomials, but this method also has a fifth-order error and is more complex to implement.

To approximate the integral of a function f over an interval $[a, b]$, the interval is divided into n equal subintervals, each with a length of $h = \frac{b-a}{n}$. The endpoints of each division are provided by $l_i = a + ih$ with $i = 0, 1, \ldots, n$. For Simpson's 1/3 rule, n is an even number, and the integral of f can be expressed as:

$$\int_a^b f(s)ds = \int_a^{l_2} f(s)ds + \int_{l_2}^{l_4} f(s)ds + \ldots + \int_{l_{i-1}}^{l_{i+1}} f(s)ds + \ldots + \int_{l_{n-2}}^{b} f(s)ds,\tag{15}$$

where l = points inside the interval (a, b).

Thus, each integral can be computed as:

$$\int_{l_{i-1}}^{l_{i+1}} f(s)ds \approx \frac{1}{3}h(f(l_{i-1}) + 4f(l_i) + f(l_{i+1}))\tag{16}$$

The integral of f is yielded by:

$$\int_a^b f(s)ds \approx (b - a)\frac{f(l_0) + 4\sum_{i=0}^{\frac{n-2}{2}}f(l_{2i+1}) + 2\sum_{i=1}^{\frac{n-2}{2}}f(l_{2i}) + f(l_n)}{3n},\tag{17}$$

Before applying Simpson's 1/3 rule, it is crucial to analyse the term $\left(e^{\frac{f}{D}\ (S)}(S)^{2R_v g A^2} \right)$ $\left(2\frac{p_0^*}{\rho S} - \frac{2p_{atm}^* x_0^k}{\rho S(L_T - S)^k} + 2g\ sin\ \theta \right)$ in Equation (14). The integrand in the interval $[L_0, L]$ has large values; therefore, when performing the integration, the numbers become substantial, potentially causing memory issues for computers. Equation (18) reflects this situation:

$$z = \int_{L_0}^{L} \left(e^{\frac{f}{D}\ (S)}(S)^{2R_v g A^2} \right) \left(2\frac{p_0^*}{\rho S} - \frac{2p_{atm}^* x_0^k}{\rho S(L_T - S)^k} + 2g\ sin\ \theta \right) dS, \quad (18)$$

In this context, the integrand is formulated as:

$$z = \int_{L_0}^{L} \left(\frac{1}{e^{\frac{f}{D}L}\ L^{2R_v g A^2}} \right) \left(e^{\frac{f}{D}\ (S)}(S)^{2R_v g A^2} \right) \left(2\frac{p_0^*}{\rho S} - \frac{2p_{atm}^* x_0^k}{\rho S(L_T - S)^k} + 2g\ sin\ \theta \right) dS, \quad (19)$$

By substituting Equation (17) into Equation (19) to find the value of z, thus:

$$
\begin{aligned}
z \cong \frac{f}{3nD}(L - L_0) &\left[\left(\frac{1}{e^{\frac{f}{D}L}\ L^{2R_v g A^2}} \right) \left(e^{\frac{f}{D}\ (L_0)}(L_0)^{2R_v g A^2} \right) \left(2\frac{p_0^*}{\rho L_0} - \frac{2p_{atm}^* x_0^k}{\rho L_0(L_T - L_0)^k} + 2g\ sin\ \theta \right) \right. \\
&+ 4 \sum_{i=0}^{(n-2)/2} \left(\frac{1}{e^{\frac{f}{D}L}\ L^{2R_v g A^2}} \right) \left(e^{\frac{f}{D}\ (l_{2i+1})}(l_{2i+1})^{2R_v g A^2} \right) \left(2\frac{p_0^*}{\rho l_{2i+1}} - \frac{2p_{atm}^* x_0^k}{\rho l_{2i+1}(L_T - l_{2i+1})^k} + 2g\ sin\ \theta \right) \\
&+ 2 \sum_{i=1}^{(n-2)/2} \left(\frac{1}{e^{\frac{f}{D}L}\ L^{2R_v g A^2}} \right) \left(e^{\frac{f}{D}\ (l_{2i})}(l_{2i})^{2R_v g A^2} \right) \left(2\frac{p_0^*}{\rho l_{2i}} - \frac{2p_{atm}^* x_0^k}{\rho l_{2i}(L_T - l_{2i})^k} + 2g\ sin\ \theta \right) \\
&+ \left. \left(\frac{1}{e^{\frac{f}{D}L}\ L^{2R_v g A^2}} \right) \left(e^{\frac{f}{D}\ (L)}(S)^{2R_v g A^2} \right) \left(2\frac{p_0^*}{\rho L} - \frac{2p_{atm}^* x_0^k}{\rho S(L_T - L)^k} + 2g\ sin\ \theta \right) \right]
\end{aligned}
\quad (20)
$$

where n refers to the number of parts of the interval $[a, b]$.

The complete resolution of the system is provided by Equations (14) and (19).

2.3. Methodology

This section outlines the methodology this research uses, structured into five steps, as depicted in Figure 2. The input data pertain to practical applications of a water pipeline start-up typically conducted by water utilities. This initial step requires topological characteristics of pipelines and initial conditions of hydraulic and thermodynamic variables (such as water velocity, air pocket pressure, and water column length).

The case study is modelled using two formulations: (i) the mathematical model simulating the filling process through the RCM, the polytropic law, and the piston formula and (ii) the proposed approach developed in this research, which simplifies the current mathematical model. The numerical resolution was carried out using Octave v7.1.0 software, with the ODE45 function (Runge–Kutta method) employed to solve the proposed approach's numerical and analytical aspects. A sensitivity analysis of parameters is conducted to observe their influence on the responses of the proposed approach. Similarly, the results from the proposed approach are compared with those from the mathematical model. Finally, the section concludes with a discussion of the results obtained.
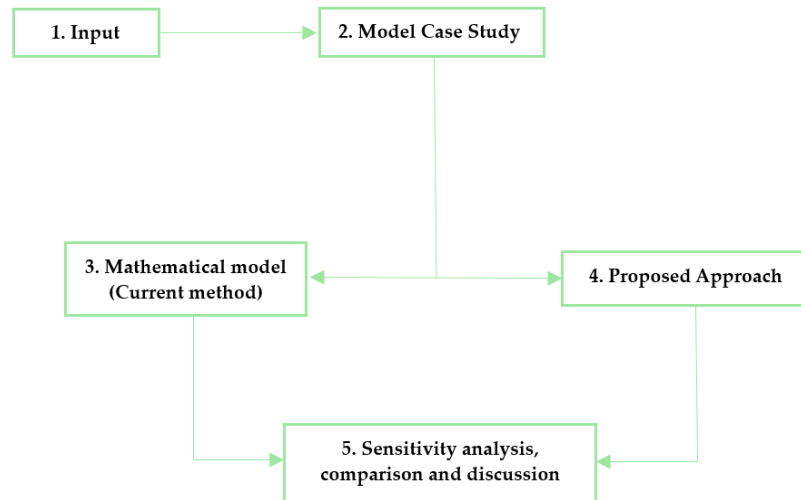
```
┌──────────────┐          ┌────────────────────┐
│  1. Input    │─────────▶│ 2. Model Case Study│
└──────────────┘          └────────────────────┘


┌────────────────────┐              ┌────────────────────┐
│ 3. Mathematical    │◀────────────▶│ 4. Proposed        │
│ model (Current     │              │    Approach        │
│ method)            │              └────────────────────┘
└────────────────────┘

              ┌────────────────────────┐
              │ 5. Sensitivity analysis,│
              │ comparison and          │
              │ discussion              │
              └────────────────────────┘
```

Figure 2. Research methodology employed.

3. Analysis of Results

This section presents the application of the proposed approach to a case study involving a filling process. The data for the case study are as follows: an initial air pocket size (x_0) of 400 m, an internal pipe diameter (D) of 0.4 m, a total length (L_T) of 600 m, a constant friction factor (f) of 0.018, an intermediate condition of polytropic evolution ($k = 1.2$), a longitudinal slope (θ) of 0.019 rad, and an initial pressure (p_0^*) of 202,650 Pa. This case study is referred to as the "baseline solution" in the following sections.

Figure 3 shows the results of the filling operation based on the proposed approach. This procedure is only applicable until the process reaches the first instance of zero water velocity, corresponding to when the air pocket pressure reaches its maximum value in this transient event. The proposed approach can be used to compute the maximum values of extreme variables (water velocity, air pocket pressure, and length of a water column). In this scenario, the initial size of the water column is 200 m when the system is at rest. The maximum water velocity is 4.77 m/s, which occurs when the water column length is 251.78 m. The highest peak in the air pocket pressure head is 33.59 m, which occurs when the water column length is 450.29 m. This is crucial, since the proposed approach can compute the extreme value during this process, which must be considered when selecting a suitable pipe resistance class.
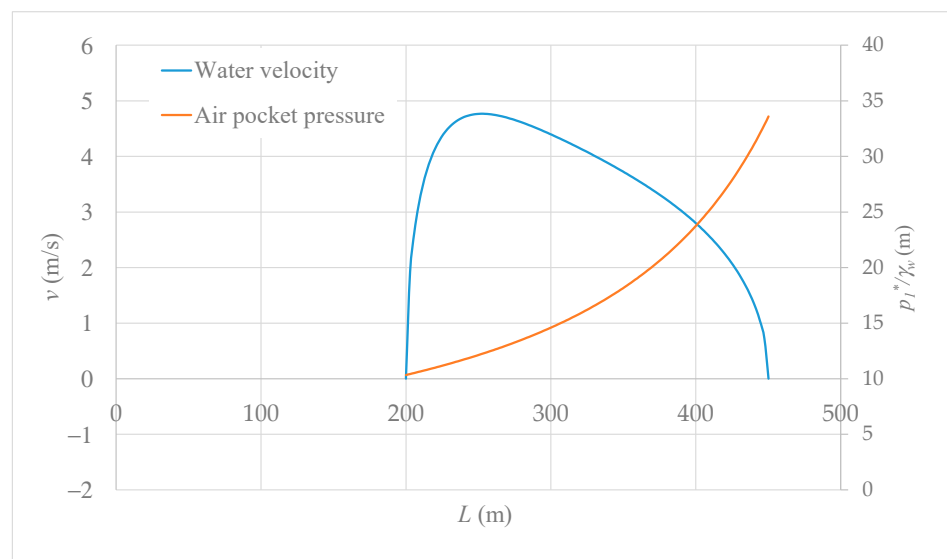

Figure 3. Results of the filling operation using the proposed approach.

Some parameters' influences were analysed to observe the responses of the proposed approach. Table 1 shows the range of variation in the analysed parameters.

Table 1. The range of parameters analysed.

Parameter	Units	Range	
		From	**To**
Internal pipe diameter (D)	m	0.2	0.5
Friction factor (f)	(-)	0.010	0.022
Longitudinal slope (θ)	rad	0.010	0.050
Polytropic coefficient (k)	(-)	1.0	1.4
Air pocket size (x_0)	m	200	500

The variation in parameters is analysed based on the results presented in Figure 3. Figure 4 illustrates the influence of internal pipe diameter, friction factor, and longitudinal slope. These variables exhibit a similar trend; therefore, the maximum value of the air pocket pressure head is analysed.
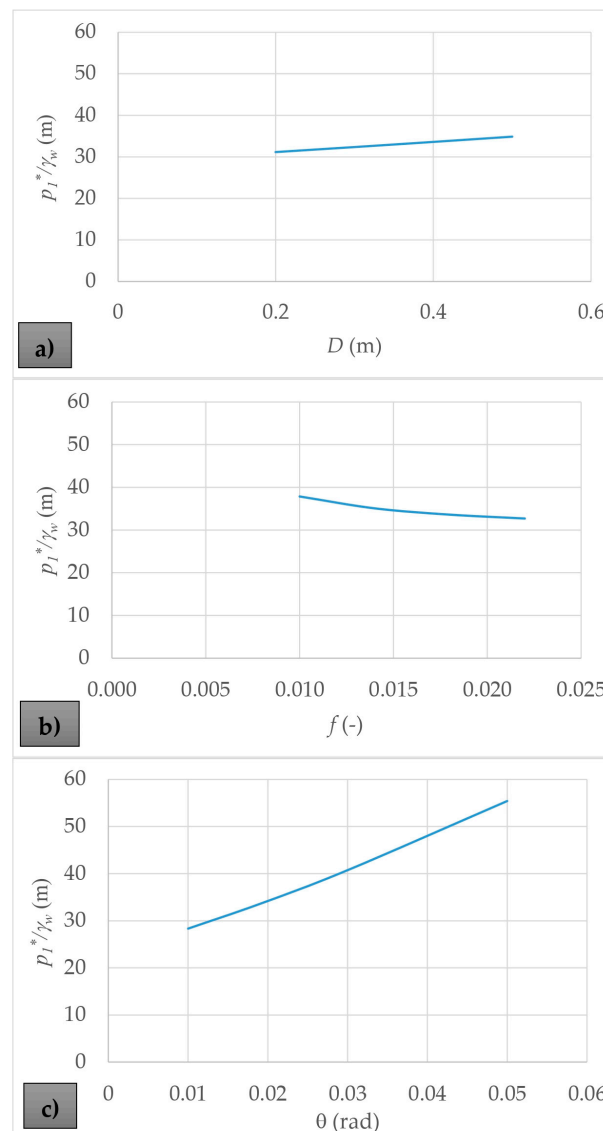

Figure 4. Influence of hydraulic and thermodynamic variables on maximum values in air pocket pressure head: (**a**) internal pipe diameter; (**b**) friction factor; and (**c**) longitudinal slope.

The internal pipe diameter varied from 0.2 to 0.5 m. As the pipe diameter increases, the air pocket pressure head rises due to the greater water volume in the system, as shown in Figure 4a. The air pocket pressure head varies from 31.15 to 34.85 m.

The friction factor is analysed from 0.010 to 0.022 (Table 1). The results indicate that a higher friction factor produces a lower air pocket pressure head (see Figure 4b). For instance, with a friction factor of 0.010, an air pocket pressure head peak of 37.86 m is achieved, while with a friction factor of 0.022, a value of 32.69 m is observed.

Another critical parameter is the longitudinal pipe slope. Its influence is analysed as shown in Figure 4c. The higher the longitudinal pipe slope, the greater the values in air pocket pressure attained. Air pocket pressure heads vary from 28.35 to 55.38 m for longitudinal slopes of 0.010 and 0.050 radians, respectively.

The transient event is analysed considering the variation in the air pocket size and polytropic coefficient, as shown in Figure 5. An isothermal evolution ($k = 1.0$) shows greater values compared to adiabatic ($k = 1.4$) and intermediate ($k = 1.2$) behaviours. The maximum value of the air pocket pressure head during the transient event for an isothermal evolution is 34.28 m, while for adiabatic behaviour, 33.17 m is computed (see Figure 5a). Figure 5b presents the air pocket pressure graph versus the water column length, considering air pocket sizes of 200, 300, 400, and 500 m. As expected, the smaller the air pocket size, the higher the peak in air pocket pressure attained according to the polytropic law. Specifically, for an initial air pocket size of 200 m, a maximum air pocket pressure head of 41.26 m is reached. In comparison, for an initial air pocket size of 500 m, the maximum value is 31.51 m. Figure 5b shows the results when the air pocket size is varied.
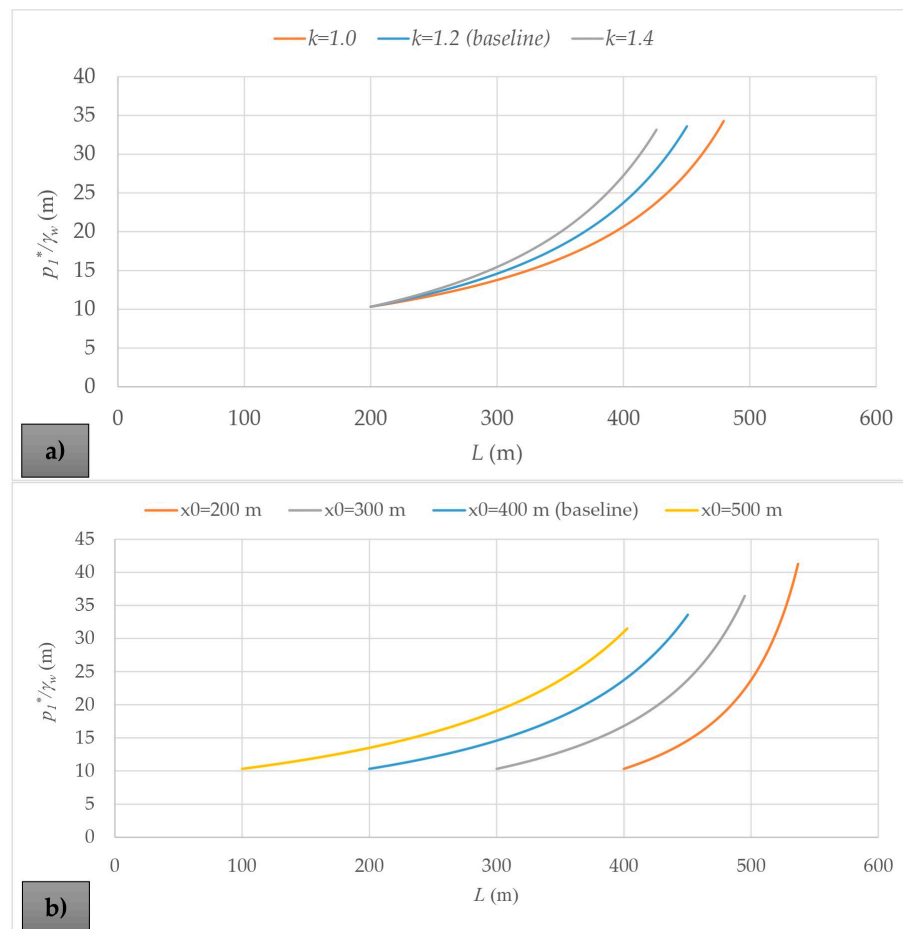

Figure 5. Analysis of hydraulic transient: (**a**) polytropic coefficient and (**b**) air pocket size.

4. Discussion

4.1. Comparison with a 1D Mathematical Model

The proposed approach can be applied from the beginning of the transient flow until the water velocity first reaches a null value. At this point, the maximum value of the air pocket pressure is achieved. Figure 6 presents the complete resolution (mathematical model) of the water pipeline start-up, considering Equations (1), (3), and (4), compared to the solution provided by the proposed approach. The mathematical model (grey and green lines) is suitable for simulating the complete transient event, as shown in Figure 6. Although the proposed approach (blue and orange lines) only presents the simulation until the water velocity reaches 0 m/s, it is sufficient for practical application, since the maximum peak in air pocket pressure is reached. Based on this value, engineers and designers can select an appropriate pipe resistance class. The proposed approach can reproduce the maximum value in air pocket pressure head of 33.59 m and the maximum value of water velocity of 4.77 m/s. These results coincide with the mathematical model, as presented in Figure 6.
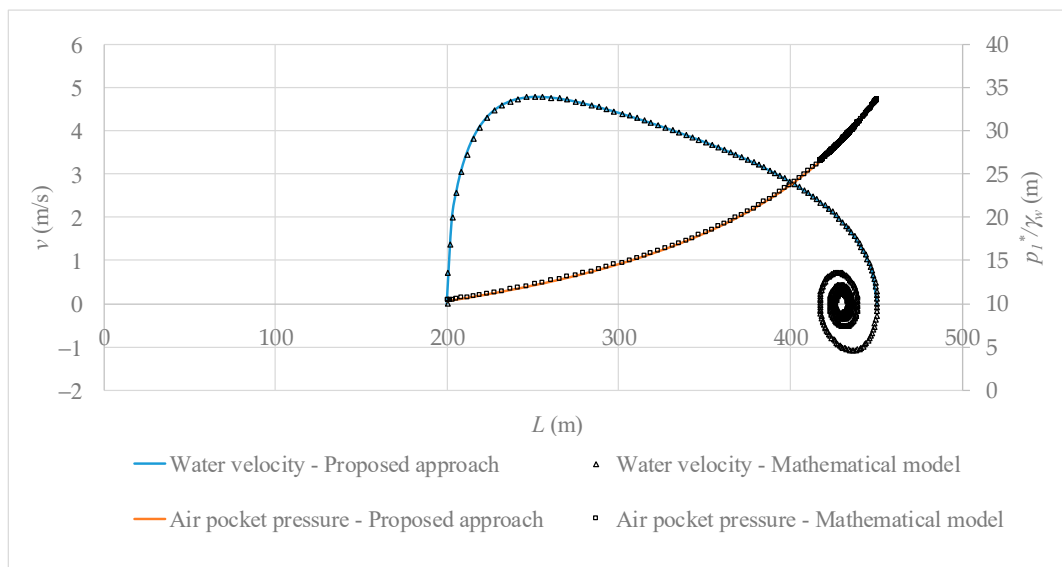

Figure 6. Comparison between the complete numerical resolution and the proposed approach.

4.2. Analysis of the Number of Intervals in the Proposed Approach

The number of intervals (n) for integrating the integral I was analysed, considering both even and odd numbers, as presented in Figure 7. Figure 7a shows the solution for even numbers 2, 6, 10, and 30. The case study was conducted with $n = 30$. The results indicate that the proposed approach achieves better accuracy as the number of intervals increases. For instance, with $n = 2$, the proposed approach tends to find the maximum value of the air pocket pressure head. Additionally, the maximum value of water velocity is adequately computed by the proposed approach using $n = 2$.

When an odd number of intervals is used, the proposed approach can compute the final value of the air pocket pressure head (33.59 m). However, it is not suitable for accurately representing the evolution of the transient event, as shown in Figure 7b, where n takes values of 5, 7, and 30 (baseline). This suggests that implementing the proposed approach should be carried out using an even number of intervals, as Simpson's 1/3 rule is defined under this condition.

Figure 8 shows the results of the integrand *I* considering Equations (18) and (19). For the case study, the reformulated equation to compute the integrand (Equation (19)) ensures appropriate values for evaluating the integral, avoiding large numbers. Implementing Equation (18) yields values of magnitude greater than -10^7.
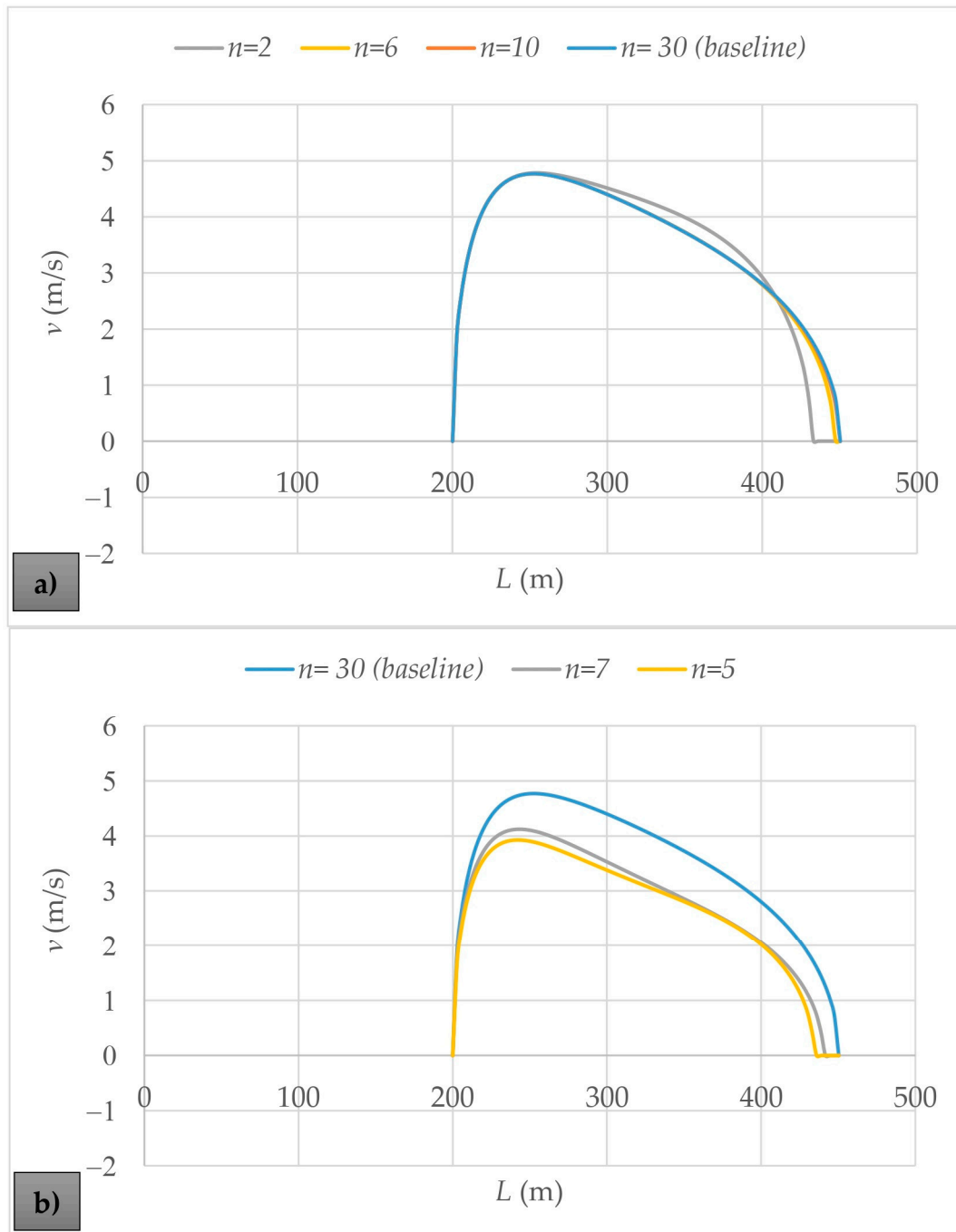

Figure 7. Analysis of the number of intervals (*n*) to integrate *I*: (**a**) using an even number of intervals and (**b**) using an odd number of intervals.
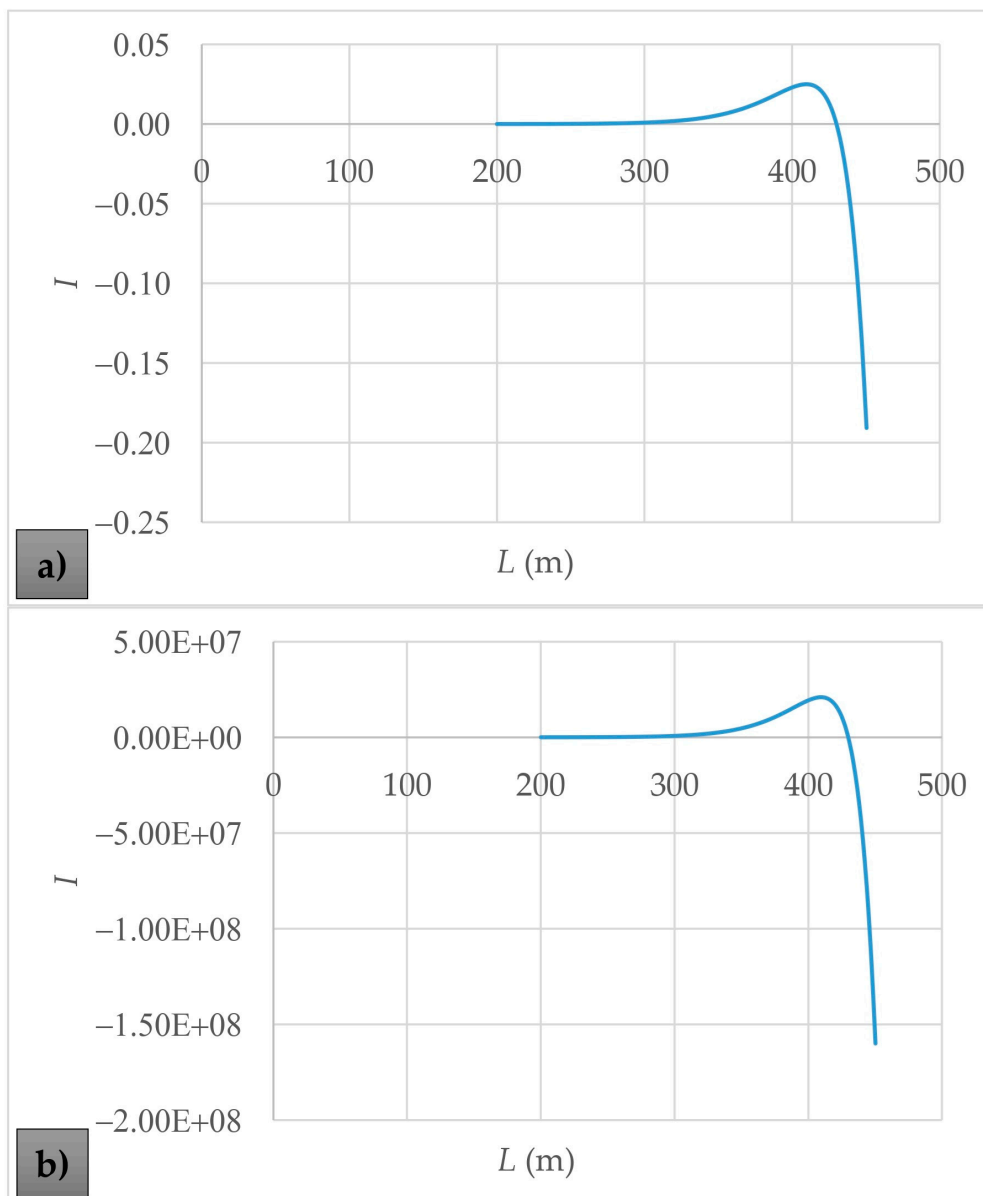
Figure 8. Analysis of integrand *I* using: (**a**) Equation (19) and (**b**) Equation (18).

4.3. Validation

The proposed approach is derived from the mathematical model presented in Section 2. Moreover, as illustrated in Figure 6, both models produce identical results for an instantaneous opening of regulating valves. The primary advantage of the proposed method is its ability to enable water utilities to calculate the maximum air pocket pressure in water pipelines rapidly. The proposed approach assumes an instantaneous valve opening, expected to yield higher values than scenarios involving gradual valve openings. In this context, the authors utilised the experimental data provided by Bonilla-Correa et al. (2023) [15]. The experimental setup consists of a 7.36 m long inclined pipeline with a nominal diameter of 63 mm and a pipe slope of $30°$. The resistance coefficient (R_v) for a fully open valve was 17,000 ms^2/m^6. For the analysis, two air pockets (x_0) of 0.96 and 1.36 m were considered, with the initial pressure head (p_0^*) varying between 1.75 and 2.25 bar. Table 2 presents the experimental measurements.

Table 2. Experimental tests.

Test No.	p_0^*(bar)	x_0 (m)
1	1.75	0.96
2	1.75	1.36
3	2.25	0.96
4	2.25	1.36

The proposed approach was tested using the experimental measurements presented in Table 2. Figure 9 compares the computed and measured maximum air pocket pressure head for the tests analysed. The proposed approach is expected to yield higher air pocket pressure values than the exact solution, as the experimental tests involved a gradual manoeuvre. An electro-pneumatic valve with a 0.2-s aperture was used during the experiments.
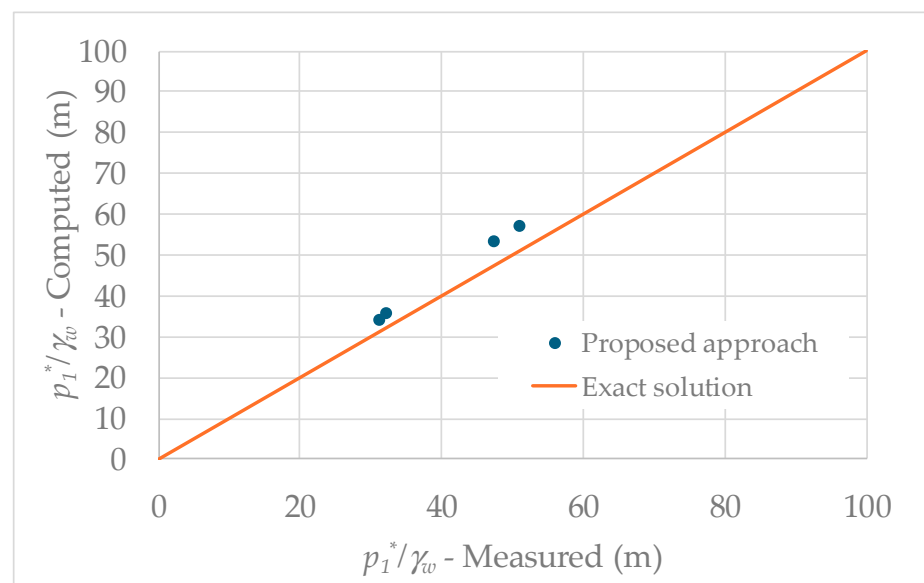

Figure 9. Comparison between computed and measured maximum air pocket pressure.

To assess the accuracy of the proposed approach, the root mean square error (*RMSE*) and the correlation coefficient (R^2) were calculated as follows:

$$RMSE = \sqrt{\frac{1}{N}\sum_{j=1}^{N}\left(p_{1,computed,j}^* - p_{1,measured,j}^*\right)^2}, \tag{21}$$

where $p_{1,computed}^*$ = air pocket pressure computed by the proposed approach, $p_{1,measured}^*$ = measured air pocket pressure, and N = total number of tests analysed.

$$R^2 = \frac{\sum_{j=1}^{N}\left(p_{1,computed,j}^* - \overline{p_{1,computed}^*}\right)\left(p_{1,measured,j}^* - \overline{p_{1,measured}^*}\right)}{\sqrt{\sum_{j=1}^{N}\left(p_{1,computed,j}^* - \overline{p_{1,computed}^*}\right)^2}\sqrt{\sum_{j=1}^{N}\left(p_{1,measured,j}^* - \overline{p_{1,measured}^*}\right)^2}}, \tag{22}$$

Based on the results presented in Figure 9, the RMSE and R² values are 4.72 m and 0.99, respectively. This indicates that the proposed approach is well suited for application in water utilities, as it closely aligns with the experimental results, even when not accounting for a gradual manoeuvre.

4.4. Comparison with Previous Models

Water utilities can utilise the proposed approach to calculate the maximum air pocket pressure during filling operations, particularly when considering an instantaneous valve-opening manoeuvre. This scenario is more critical, as it produces the highest pressure surges. The proposed approach can yield results comparable to 1D, 2D, and 3D models [3]. Implementing 1D models is complex, necessitating the numerical solution of partial and ordinary differential equations when formulating the elastic and rigid water models [15,20]. These models are well suited for capturing both rapid and slow valve-opening manoeuvres. The 2D and 3D CFD models provide a more intricate solution, allowing for detailed consideration of thermodynamic and hydraulic variables [3,24]. However, these models demand significantly higher computational resources than 1D models and the proposed approach.

5. Conclusions

This paper introduces an approach for computing water pipeline start-ups involving entrapped air pockets. The proposed approach simplifies an existing 1D mathematical model developed by the authors which incorporates the rigid column model, the polytropic law, and the piston flow equation to simulate the air–water interface. It is valid until the system reaches zero water velocity during the transient event.

The proposed approach is beneficial for determining the maximum value of an air pocket pressure head during a filling operation. It is paramount, as the proposed approach represents the sole analytical-numerical equation developed from physical equations in the current literature. The results of the proposed approach can be used to verify whether the pipe resistance class was appropriately selected, enhancing system feasibility. It is a practical tool that can be used for water utilities to evaluate extreme pressure with entrapped air pockets in pipelines. Its implementation is more accessible than rigid- and elastic-column models. The proposed approach is based on an analytical resolution, which includes an integrand that needs to be solved numerically using Simpson's 1/3 rule.

A practical application was tested using a 600 m long pipeline with an internal diameter of 400 mm. A sensitivity analysis of varying parameters such as pipe diameter, friction factor, longitudinal slope, polytropic coefficient, and air pocket size was conducted. The proposed approach yielded values consistent with the current mathematical model.

Furthermore, the proposed model was compared with the 1D mathematical model, demonstrating that both models accurately predict extreme air pocket pressure heads. This confirms that the proposed approach can be considered reliable for selecting the pipe resistance class. A sensitivity analysis was also performed on Simpson's 1/3 rule, showing that the proposed approach maintains good accuracy under the specified assumptions.

The proposed approach involves an instantaneous opening manoeuvre in regulating valves, enabling the computation of the maximum air pocket pressure. Water utilities can use this information to select the appropriate pipe resistance class for pipelines. The approach was validated using experimental measurements conducted on a 7.36 m long pipeline with a nominal diameter of 63 mm.

The proposed approach should be tested on more complex pipeline networks for future work. Additionally, its implementation should be incorporated into commercial software packages for filling operations.

Conflicts of Interest: The authors declare no conflicts of interest.

Nomenclature

The following abbreviations were used in this manuscript:

Variables

A:	cross-sectional area of a pipe (m^2)
D:	internal pipe diameter (m)
g:	gravitational acceleration (m/s^2)
$h(L)$:	function that depends on some variables (-)
k:	polytropic coefficient (-)
I:	integral
L:	length of a water column (m)
l:	points inside the interval (a, b) (-)
L_T:	pipe length (m)
n:	refers to the number of parts of an interval $[a, b]$ (-).
p_0^*:	pressure provides by an energy source (Pa)
p_{atm}^*:	atmospheric pressure (101,325 Pa)
p_1^*:	air pocket pressure (Pa)
R_v:	resistance coefficient of a regulating valve (ms^2/m^6)
s:	variable of integration
v:	water velocity (m/s)
x:	air pocket size (m)
z:	water velocity square (m^2/s^2)
θ:	longitudinal slope (rad)
ρ:	water density (kg/m^3)
γ_w:	water unit weight (N/m^3)

Subscripts

0:	refers to an initial condition

Acronyms

ECM	elastic-column model
RCM	rigid-column model

References

1. Izquierdo, J.; Fuertes, V.S.; Cabrera, E.; Iglesias, P.L.; Garcia-Serra, J. Pipeline Start-up with Entrapped Air. *J. Hydraul. Res.* **1999**, *37*, 579–590. [CrossRef]
2. Li, H.; Bai, C.; Wang, J. Experiments and Numerical Analysis of the Dynamic Flow Characteristics of a Pump−pipeline System with Entrapped Air during Start-Up. *Eng. Appl. Comput. Fluid Mech.* **2023**, *17*, 2238853. [CrossRef]
3. Fuertes-Miquel, V.S.; Coronado-Hernández, O.E.; Mora-Meliá, D.; Iglesias-Rey, P.L. Hydraulic Modeling during Filling and Emptying Processes in Pressurized Pipelines: A Literature Review. *Urban Water J.* **2019**, *16*, 299–311. [CrossRef]
4. Vasconcelos, J.G.; Wright, S.J. Investigation of Rapid Filling of Poorly Ventilated Stormwater Storage Tunnels. *J. Hydraul. Res.* **2009**, *47*, 547–558. [CrossRef]
5. Zhou, F.; Hicks, F.E.; Steffler, P.M. Transient Flow in a Rapidly Filling Horizontal Pipe Containing Trapped Air. *J. Hydraul. Eng.* **2002**, *128*, 625–634. [CrossRef]
6. Tijsseling, A.S.; Hou, Q.; Bozkuş, Z.; Laanearu, J. Improved One-Dimensional Models for Rapid Emptying and Filling of Pipelines. *J. Press. Vessel Technol.* **2015**, *138*, 031301. [CrossRef]
7. Zhou, L.; Liu, D.; Ou, C. Simulation of Flow Transients in a Water Filling Pipe Containing Entrapped Air Pocket with VOF Model. *Eng. Appl. Comput. Fluid Mech.* **2011**, *5*, 127–140. [CrossRef]
8. He, J.; Hou, Q.; Lian, J.; Tijsseling, A.S.; Bozkus, Z.; Laanearu, J.; Lin, L. Three-Dimensional CFD Analysis of Liquid Slug Acceleration and Impact in a Voided Pipeline with End Orifice. *Eng. Appl. Comput. Fluid Mech.* **2022**, *16*, 1444–1463. [CrossRef]
9. Malekpour, A.; Karney, B.W.; Nault, J. Physical Understanding of Sudden Pressurization of Pipe Systems with Entrapped Air: Energy Auditing Approach. *J. Hydraul. Eng.* **2016**, *142*, 04015044. [CrossRef]
10. Abreu, J.; Cabrera, E.; Izquierdo, J.; García-Serra, J. Flow Modeling in Pressurized Systems Revisited. *J. Hydraul. Eng.* **1999**, *125*, 1154–1169. [CrossRef]

11. Wan, W.; Zhang, B.; Chen, X. Investigation on Water Hammer Control of Centrifugal Pumps in Water Supply Pipeline Systems. *Energies* **2019**, *12*, 108. [CrossRef]

12. Biao, H.; Zhu, Z.D. Rigid-Column Model for Rapid Filling in a Partially Filled Horizontal Pipe. *J. Hydraul. Eng.* **2021**, *147*, 06020018. [CrossRef]

13. Paternina-Verona, D.A.; Coronado-Hernández, O.E.; Espinoza-Román, H.G.; Arrieta-Pastrana, A.; Tasca, E.; Fuertes-Miquel, V.S.; Ramos, H.M. Attenuation of Pipeline Filling Over-Pressures through Trapped Air. *Urban Water J.* **2024**, *21*, 698–710. [CrossRef]

14. Wang, J.; Vasconcelos, J.G. Investigation of Manhole Cover Displacement during Rapid Filling of Stormwater Systems. *J. Hydraul. Eng.* **2020**, *146*, 4020022. [CrossRef]

15. Bonilla-Correa, D.M.; Coronado-Hernández, Ó.E.; Fuertes-Miquel, V.S.; Besharat, M.; Ramos, H.M. Application of Newton–Raphson Method for Computing the Final Air–Water Interface Location in a Pipe Water Filling. *Water* **2023**, *15*, 1304. [CrossRef]

16. Zhou, L.; Liu, D.; Karney, B.; Zhang, Q. Influence of Entrapped Air Pockets on Hydraulic Transients in Water Pipelines. *J. Hydraul. Eng.* **2011**, *137*, 1686–1692. [CrossRef]

17. Ferras, D.; Manso, P.A.; Schleiss, A.J.; Covas, D.I. One-dimensional fluid–structure interaction models in pressurized fluid-filled pipes: A review. *Appl. Sci.* **2018**, *8*, 1844. [CrossRef]

18. Feng, Y.; Yi, H.; Liu, R. Analytical Solution for Transient Electroosmotic and Pressure-Driven Flows in Microtubes. *Fluids* **2024**, *9*, 140. [CrossRef]

19. Tijsseling, A.S.; Hou, Q.; Bozkuş, Z. Rapid Liquid Filling of a Pipe With Venting Entrapped Gas: Analytical and Numerical Solutions. *J. Press. Vessel Technol.* **2019**, *141*, 041301. [CrossRef]

20. Zhou, L.; Liu, D.; Karney, B.; Wang, P. Phenomenon of White Mist in Pipelines Rapidly Filling with Water with Entrapped Air Pockets. *J. Hydraul. Eng.* **2013**, *139*, 1041–1051. [CrossRef]

21. Coronado-Hernández, Ó.E.; Besharat, M.; Fuertes-Miquel, V.S.; Ramos, H.M. Effect of a Commercial Air Valve on the Rapid Filling of a Single Pipeline: A Numerical and Experimental Analysis. *Water* **2019**, *11*, 1814. [CrossRef]

22. Martin, C.S. Entrapped Air in Pipelines. 1977.

23. Budak, H.; Hezenci, F.; Kara, H.; Sarikaya, M.Z. Bounds for the Error in Approximating a Fractional Integral by Simpson's Rule. *Mathematics* **2023**, *11*, 2282. [CrossRef]

24. Huang, B.; Fan, M.; Liu, J.; Zhu, D.Z. CFD Simulation of Air–Water Interactions in Rapidly Filling Horizontal Pipe with Entrapped Air. In Proceedings of the World Environmental and Water Resources Congress, Virtual, 7–11 June 2021; pp. 495–507. [CrossRef]